

A fluorescent variant of a protein from the stony coral *Montipora* facilitates dual-color single-laser fluorescence cross-correlation spectroscopy

Takako Kogure¹, Satoshi Karasawa¹⁻³, Toshio Araki¹⁻³, Kenta Saito⁴, Masataka Kinjo⁴ & Atsushi Miyawaki¹

Dual-color fluorescence cross-correlation spectroscopy (FCCS) is a promising technique for quantifying protein-protein interactions¹⁻⁵. In this technique, two different fluorescent labels are excited and detected simultaneously within a common measurement volume. Difficulties in aligning two laser lines and emission crossover between the two fluorophores, however, make this technique complex. To overcome these limitations, we developed a fluorescent protein with a large Stokes shift. This protein, named Keima, absorbs and emits light maximally at 440 nm and 620 nm, respectively. Combining a monomeric version of Keima with cyan fluorescent protein allowed dual-color FCCS with a single 458-nm laser line and complete separation of the fluorescent protein emissions. This FCCS approach enabled sensitive detection of proteolysis by caspase-3 and the association of calmodulin with calmodulin-dependent enzymes. In addition, Keima and a spectral variant that emits maximally at 570 nm might facilitate simultaneous multicolor imaging with single-wavelength excitation.

Dual-color FCCS has several advantages over standard fluorescence correlation spectroscopy (FCS). Whereas FCS detects molecular concentrations and mobility³, FCCS enables the tracing of two spectrally distinguishable fluorophores, thus extracting essential information about the kinetics of molecular interactions¹⁻⁵. FCCS requires two fluorophores of different colors. For simultaneous excitation of the two fluorophores, two lasers are aligned to the same confocal spot. Bringing two laser beams to a perfect and stable overlap, however, is often difficult. Although FCCS can be performed using a single laser line (SL-FCCS) for single-photon excitation⁶, complex mathematical computations are required to compensate for cross-excitation, cross-talk and fluorescence resonance energy transfer (FRET) when common fluorophores that have broad excitation and emission spectra and modest Stokes shifts are used. Thus, simple SL-FCCS has been achieved only with special fluorophores, such as 'MegaStokes' dyes (<http://www.dyomics.com/>), although some innovative techniques for specific labeling of recombinant proteins with organic dyes⁷ might

render the MegaStokes dyes more applicable. One solution for efficient simultaneous excitation may come from two-photon excitation (TPE) microscopy⁸; two differently colored fluorophores can be excited simultaneously by a single infrared, ultra-short pulse laser line because of the blue-shift effect. Although TPE-SL-FCCS performs well⁹⁻¹², it requires expensive equipment and specialized expertise. Also, in TPE, the rate of bleaching per unit excitation increases supralinearly with pulse intensity^{13,14}. This increase may add another decay component, thereby complicating analyses.

The development of fluorescent proteins with large Stokes shifts has long been pursued to create a fluorescent protein pair in which the two fluorescent proteins have comparable excitation maxima but sufficiently different Stokes shifts. To identify such candidate proteins, we used degenerate primers¹⁵ to amplify cDNAs constructed from the stony coral *Montipora* sp. One clone was selected that encoded a new green fluorescent protein (GFP)-like protein. The protein, referred to as no. 20, is a violet-colored chromoprotein that does not fluoresce. Its absorption spectrum at pH 7.4 shows a major absorption maximum at 576 nm ($\epsilon = 64,000 \text{ M}^{-1} \text{ cm}^{-1}$) with a slight shoulder at $\sim 535 \text{ nm}$ (Fig. 1a). Sequence analysis revealed that no. 20 is closely related to a chromoprotein from *Goniopora tenuidens* gtCP¹⁶. An amino-acid alignment of no. 20 with DsRed is shown in **Supplementary Fig. 1** online.

To efficiently evolve the chromoprotein into a useful fluorescent protein, we carried out semi-random mutagenesis¹⁷. Random substitutions of several amino acids whose side chains were close to the chromophore were simultaneously introduced into the protein. Five substitutions (H94N, N142S, N157D, K202R and F206S) and the addition of a valine residue at the second amino-acid position resulted in a red fluorescent protein (no. 20-9115). This protein showed an emission spectrum peaking at 606 nm and a bimodal excitation spectrum peaking at 452 and 580 nm (Fig. 1b). A pH titration experiment revealed that the two excitation peaks corresponded to the neutral and ionized states of the phenolic hydroxyl moiety of the chromophore, respectively¹⁸ (data not shown). To simplify the excitation spectrum, we used semi-random mutagenesis to shift the neutralization/ionization equilibrium to either of the two states. A new

¹Laboratory for Cell Function and Dynamics, Advanced Technology Development Group, Brain Science Institute, RIKEN, 2-1 Hirosawa, Wako-city, Saitama, 351-0198, Japan. ²Amalgam Co., Ltd. 2-9-3 Itabashi, Itabashi-ku, Tokyo, 173-0004, Japan. ³Medical & Biological Laboratories Co., Ltd., 3-5-10 Marunouchi, Naka-ku, Nagoya-city, 460-0002, Japan. ⁴Research Institute for Electronic Science, Hokkaido University, Sapporo, 060-0812, Japan. Correspondence should be addressed to A.M. (matsushi@brain.riken.jp).

Received 18 November 2005; accepted 29 March 2006; published online 30 April 2006; doi:10.1038/nbt1207

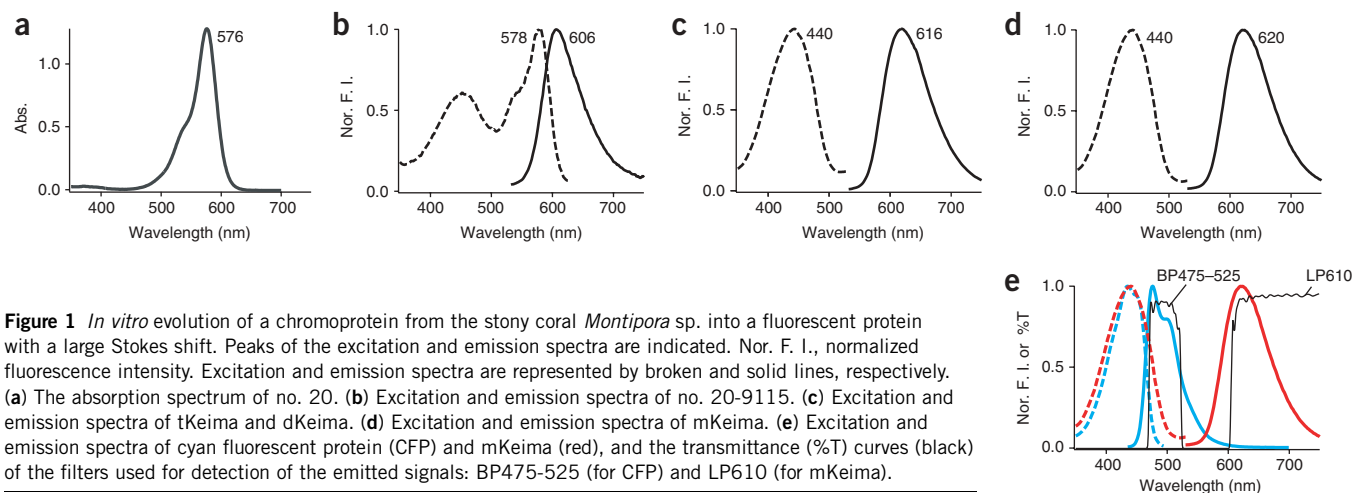


Figure 1 *In vitro* evolution of a chromoprotein from the stony coral *Montipora* sp. into a fluorescent protein with a large Stokes shift. Peaks of the excitation and emission spectra are indicated. Nor. F. I., normalized fluorescence intensity. Excitation and emission spectra are represented by broken and solid lines, respectively. (a) The absorption spectrum of no. 20. (b) Excitation and emission spectra of no. 20-9115. (c) Excitation and emission spectra of tKeima and dKeima. (d) Excitation and emission spectra of mKeima. (e) Excitation and emission spectra of cyan fluorescent protein (CFP) and mKeima (red), and the transmittance (%T) curves (black) of the filters used for detection of the emitted signals: BP475-525 (for CFP) and LP610 (for mKeima).

fluorescent protein with four mutations (S61F, I92T, F158Y and S213A) seemed to exist principally in the neutral state; the 580-nm peak was substantially reduced. Additionally, compared with those of no. 20-9115, the excitation peak of the neutral state and the emission peak were slightly blue-shifted and red-shifted, respectively. As a result, the protein absorbs light maximally at 440 nm and emits a far-red fluorescence maximally at 616 nm (Fig. 1c). Owing to the large Stokes shift, we named the protein 'Keima,' a shogi (Japanese chess) piece that hops in the manner of the knight in chess.

The absolute molecular mass of Keima was determined to be 106 kDa by analytical equilibrium ultracentrifugation analysis (Supplementary Fig. 2a online). This value was four times larger than the 25-kDa value deduced from the primary structure of the protein, suggesting that Keima forms a homotetrameric complex (referred to hereafter as 'tKeima'). At pH 7.4, the molar extinction coefficient (ϵ) at 440 nm and fluorescence quantum yield (Φ) of tKeima were $14,500 \text{ M}^{-1} \text{ cm}^{-1}$ and 0.22, respectively. The monomeric version of DsRed was previously generated by altering 33 amino-acid residues¹⁹. Assuming that the structure of tKeima is similar to that of the DsRed tetramer, we introduced V123T into the AB interface. Another mutation (V191I) was introduced to increase the folding efficiency of the mutant. The absolute molecular mass of 52.2 kDa (Supplementary Fig. 2b) was almost twice the predicted size of the monomer. This dimeric protein was named 'dKeima.' Compared to tKeima, dKeima showed the same absorption spectrum peaking at 440 nm ($\epsilon = 24,600 \text{ M}^{-1} \text{ cm}^{-1}$), the same excitation/emission spectra (Fig. 1c) and a Φ of 0.31. After numerous cycles of semi-random mutagenesis, we successfully inhibited the formation of the AC dimer by introducing seven additional mutations (L60Q, F61L, V79E, T92S, T123E, Y188R and Y190E) to produce 'mKeima,' a monomeric protein. The absolute molecular mass of mKeima was 31 kDa

(Supplementary Fig. 2c). mKeima showed the same spectra as tKeima and dKeima except that the emission maximum was 620 nm (Fig. 1d). The ϵ at 440 nm and Φ of mKeima were $14,400 \text{ M}^{-1} \text{ cm}^{-1}$ and 0.24, respectively. The mutations introduced into no. 20 to form mKeima are summarized in Supplementary Fig. 1. Additionally, the spectral characteristics of tKeima, dKeima and mKeima are summarized in Supplementary Table 1 online.

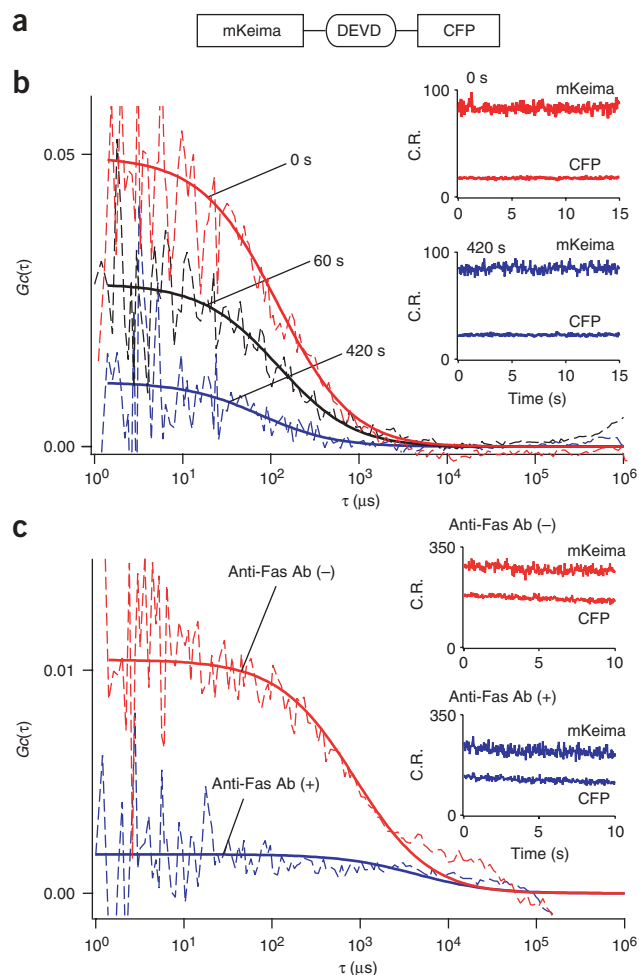


Figure 2 Single laser wavelength (458 nm) excitation FCCS using mKeima and CFP to monitor proteolysis by caspase-3. (a) A schematic representation of the primary structure of the caspase-3 sensor protein. (b) *In vitro* cross-correlation analysis. Cross-correlation curves measured at 0 s (red), 60 s (black) and 420 s (blue) after the addition of caspase-3. (c) Cross-correlation analysis in live HeLa cells. Cross-correlation curves measured from anti-Fas antibody-treated (blue) and untreated (red) cells expressing the sensor protein. (b,c) $G_c(\tau)$, the cross-correlation function. Insets: the fluorescence intensities of mKeima and CFP in the two respective channels during an FCCS measurement. C.R., count rates.

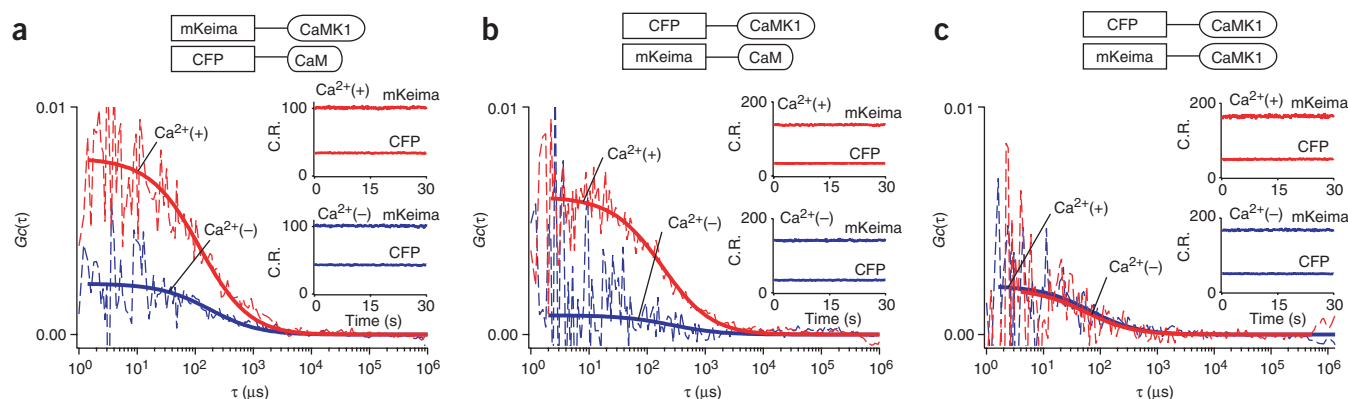


Figure 3 Single laser wavelength (458 nm) excitation FCCS using mKeima and CFP to monitor the Ca^{2+} -dependent association between CaM and CaMKI. Cross-correlation curves were measured in the presence of 0.1 mM EGTA (blue, $\text{Ca}^{2+}(-)$) and then after the addition of 1 mM CaCl_2 (red, $\text{Ca}^{2+}(+)$). $G_c(\tau)$: the cross-correlation function. Insets: the fluorescence intensities of mKeima and CFP in the two respective channels during an FCCS measurement. C.R., count rates. (a) mKeima-CaMKI and CFP-CaM. (b) CFP-CaMKI and mKeima-CaM. (c) CFP-CaMKI and mKeima-CaMKI.

We tried to establish an SL-FCCS system solely based on fluorescent proteins. Combined use of a cyan-emitting variant of *Aequorea victoria* GFP (CFP)¹⁸ and mKeima permitted simple but efficient SL-FCCS, because the two fluorescent proteins possess nearly identical excitation spectra and completely separable emission spectra (Fig. 1e). Also, there is no FRET between CFP and Keima.

The C terminus of mKeima and the N terminus of CFP (ECFP) were linked using a peptide containing the caspase-3 cleavage sequence DEVD (Fig. 2a). The recombinant protein (mKeima-DEVD-CFP) was examined in a chamber using an excitation wavelength of 458 nm. Substantial cross-correlation was observed between the fluctuations in the two detection channels (Fig. 2b, 0 s). Incubation of the same sample with activated recombinant caspase-3 (0.2 U/ μl) at 25 °C for 7 min almost completely abolished the cross-correlation signal (Fig. 2b, 420 s). The linear relationship between the relative cross-correlation and the percentage of intact substrate was verified in a

separate experiment in which several mixtures containing various ratios of intact caspase-3 substrates (mKeima-DEVD-CFP) to purified mKeima and CFP were used to measure cross-correlation signals (Supplementary Fig. 3a online). The proteolysis was then examined in apoptotic cells. The same FCCS experiments were conducted with HeLa cells transfected with cDNA coding for mKeima-DEVD-CFP. The degree of cross-correlation was substantially different between anti-Fas antibody-treated and untreated cells (Fig. 2c). It is important to note that in an mKeima-DEVD-CFP-expressing HeLa cell, mKeima and CFP were photobleached with similar kinetics during strong irradiation at 440 nm (Supplementary Fig. 3b).

Next we applied the FCCS technique to the detection of the Ca^{2+} -dependent association between calmodulin (CaM) and CaM-dependent kinase I (CaMKI). mKeima and CFP were fused to the N termini of CaMKI and CaM, respectively, to generate mKeima-CaMKI and CFP-CaM (Fig. 3a). The two fusion proteins were prepared separately using a wheat germ *in vitro* translation system. FCCS was then performed using a mixture of the two samples. The amplitude of the cross-correlation was low in the absence of Ca^{2+} (0.1 mM EGTA) (Fig. 3a, $\text{Ca}^{2+}(-)$), but increased after the addition of 1 mM CaCl_2 (Fig. 3a, $\text{Ca}^{2+}(+)$). A similar result was obtained with a combination of two alternative fusion proteins, CFP-CaMKI and mKeima-CaM (Fig. 3b). On the other hand, the cross-correlation for a mixture of CFP-CaMKI and mKeima-CaMKI was negligible irrespective of the level of Ca^{2+} (Fig. 3c). In addition, mKeima or CFP was fused to the C terminus of CaMKI or CaM to make CaMKI-mKeima, CaMKI-CFP, CaM-mKeima and CaM-CFP. Using these eight potential CaM/CaMKI combinations in FCCS experiments to monitor the association between CaM and CaMKI. A Ca^{2+} -dependent increase in cross-correlation was detected in seven of the eight combinations (see Supplementary Fig. 4 online). No increase was observed for the mixture of CaM-mKeima and

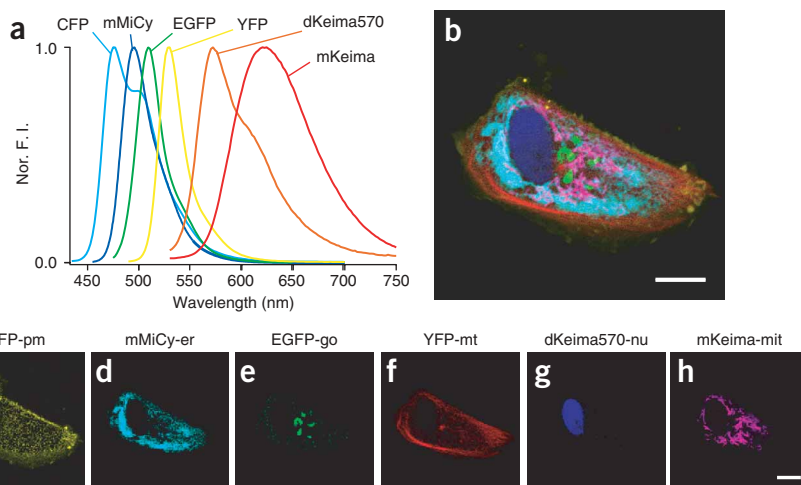


Figure 4 Simultaneous six-color imaging of subcellular structures in a Vero cell using a single laser line (458 nm). (a) Normalized emission spectra of CFP, mMiCy, EGFP, YFP, dKeima570 and mKeima. (b) An image of the Vero cell with CFP localized on the plasma membrane (yellow), mMiCy in the endoplasmic reticulum (cyan), EGFP in the Golgi (green), YFP along the microtubules (red), dKeima570 in the nucleus (dark blue) and mKeima in the mitochondria (purple). The image was created by merging the following images, which were obtained using spectral imaging: CFP-pm (c), mMiCy-er (d), EGFP-go (e), YFP-mt (f), dKeima570-nu (g) and mKeima-mit (h). Scale bars, 10 μm .

CaMKI-CFP, possibly because of disruption of the CaM/CaMKI interaction by one of the fusions. As detection of molecular associations by FCCS is usually not affected by fusion design or the size of the host proteins, this technique is applicable to high-throughput screening of interacting protein pairs. By contrast, FRET efficiency is highly sensitive to the way in which the two fluorescent proteins are fused to the host proteins; substantial effort will be required to obtain fusion constructs that give significant changes in the FRET signal upon CaM/CaMKI association.

Reversible molecular interactions should be harder to detect in live cells than in *in vitro* experiments; because cells contain endogenous unlabeled molecules, which can interfere with the association between two distinct, fluorescently labeled species, FCCS signals might be attenuated. Introducing more labeled molecules into live cells might overwhelm this interference. Unlike FRET, however, FCCS requires that the concentrations of labeled molecules are kept low to optimize the fluctuating signals. We used cell samples that had been transfected with the cDNAs for CaM-CFP and M13 (the CaM-binding peptide of myosin light chain kinase)²⁰-mKeima. Despite an excess amount of endogenous, unlabeled CaM and CaM-binding proteins, a Ca²⁺-dependent increase in the cross-correlation signal was detected (see **Supplementary Fig. 5** online), evidence for the applicability of FCCS in transfection-based experiments, which to our knowledge has not been experimentally supported before. It should be noted that the interference problem does not apply to the detection of proteolysis by FCCS, because the cross-correlation signals from double-labeled substrates should not be affected by endogenous substrates.

To test the applicability of mKeima for multicolor imaging, we simultaneously imaged the cytosolic free Ca²⁺ concentration ([Ca²⁺]_c) and mitochondrial morphology in highly motile cell samples. We cotransfected rat cardiac muscle cells with cDNAs that encoded a variant of yellow cameleon (YC3.60)²¹, a Ca²⁺ indicator containing CFP and yellow fluorescent protein (YFP)¹⁸, and a mitochondrially targeted variant of mKeima (mKeima-mit). Images of CFP, YFP and mKeima fluorescence were simultaneously acquired using a color camera (AQUACOSMOS/ASHURA, Hamamatsu Photonics) operating in the stream mode at video rate. Also, to improve the spatial resolution along the z-axis, a spinning disk unit (CSU21, Yokogawa) was placed in front of the camera. We observed contracting movement of the cell and mitochondria with contraction-coupled increases in the [Ca²⁺]_c, which was monitored using YC3.60 (see **Supplementary Fig. 6** online).

During the semi-random mutagenesis of dKeima, whose emission spectrum peaks at 616 nm, we found that two additional substitutions (F61M and Q62C) shifted the emission peak to 570 nm without affecting the excitation spectrum or dimer formation (see **Supplementary Figs. 1, 2d, 7** and **Supplementary Table 1** online). This dimeric variant was named dKeima570. We then labeled living cells with a large set of spectrally different dyes that could be excited with a single laser line. We tried to label subcellular structures in living cells with six different fluorescent proteins that can be excited at 458 nm: CFP, mMiCy²² (H. Suzuki, S.K. and A.M., unpublished data), EGFP¹⁸, YFP, dKeima570 and mKeima (**Fig. 4**). The emission spectra of these proteins overlap to various degrees (**Fig. 4a**). With the appropriate targeting signals, the fluorescent proteins were localized to the plasma membrane (CFP-pm), endoplasmic reticulum (mMiCy-er), Golgi apparatus (EGFP-go), microtubules (YFP-mt), nucleus (dKeima570-nu) or mitochondria (mKeima-mit). Vero cells expressing all six of the proteins were visualized using a 458-nm argon laser line 2 d after cotransfection. Using a commercially available confocal microscopy system, the six emission signals were precisely and efficiently separated

(**Fig. 4c-h**). An image of the superimposed signals (**Fig. 4b**) helps to clarify the dynamic interactions of subcellular structures in living cells. Thus, Keima and its variants solve longstanding problems in multi-color imaging technology, such as accurate laser alignment and excitation chromatic effects, although problems caused by emission chromatic effects have yet to be resolved.

METHODS

cDNA cloning and gene construction. A sample of the stony coral *Montipora* sp. was acquired from the ocean near the Okinawa islands by K. Iwao (Akajima Marine Science Laboratory). Total RNA was isolated from the corals by guanidine thiocyanate extraction. Synthesis, amplification using degenerate primers and generation of full-length cDNAs were carried out as previously described²³. The degenerate primers 5'-GAAGGRTGYGTCAAYGGRCAY-3' and 5'-ACVGGDCCATYDGAAGAAARTT-3' covered several regions that coded for amino-acid sequences that are conserved among GFP-like fluorescent proteins from a number of Anthozoa species¹⁵. The missing 5' and 3' ends of a cDNA fragment were amplified using the RACE strategy. cDNA encoding the protein-coding region was amplified using primers containing 5' *Bam*HI and 3' *Eco*RI sites. For bacterial expression, the digested product was then cloned in-frame into the *Bam*HI/*Eco*RI sites of pRSETB (Invitrogen). To promote efficient translation, the 5' end of the gene was modified by PCR to contain a Kozak consensus sequence (CCACCATG) after the *Bam*HI site. The *Bam*HI/*Eco*RI fragment was then subcloned into the mammalian expression vector pcDNA3 (Invitrogen).

Mutagenesis. Site-directed and semi-random mutations were introduced as described^{17,24}. Pairs of amino-acid residues that surrounded the chromophore and had side chains oriented toward the chromophore were mutated. A degenerative primer was designed for each strand so that the two residues would be randomly replaced with other amino acids. Also, multiple primer sets were used to simultaneously introduce random mutations at selected sites. *Escherichia coli* cells transformed with mutagenized plasmids were screened on agar plates for red fluorescence using the fluorescence image analyzing system described previously²⁴.

Protein expression, *in vitro* spectroscopy and pH titrations. Fluorescent proteins were expressed in *E. coli*, purified and characterized spectroscopically as previously described²³. Fluorescence quantum yields were determined using fluorescein as a standard (0.91). For the calculation of molar extinction coefficients, protein concentrations were measured using a Bradford assay kit (Bio-Rad) and bovine serum albumin as the standard. pH titrations were performed as described²³.

Analytical ultracentrifugation. Sedimentation equilibrium experiments were performed using a Beckman XL-1 analytical ultracentrifuge at 20 °C. Absorbance was measured at the maximum wavelength as a function of radius at rotor speeds of 18.1 × 10³g and 50.3 × 10³g and protein concentrations of 0.125, 0.25 and 0.5 absorbance units. Using this analytical system, the tetramerization of DsRed was verified.

FCCS. The LSM 510 META/ConfoCor 2 system (Carl Zeiss) equipped with an Ar ion laser was used. The excitation line was set at 458 nm. The excitation beam was reflected by a HFT458 dichroic mirror and focused by a water immersion objective lens (C-Apochromat 40X/NA1.2; Carl Zeiss). The emitted light was collimated and then split by a NFT570 dichroic mirror. Emission signals were detected through a BP475-525 emission filter for CFP and a LP610 emission filter for mKeima. The transmittance curves of the two emission filters are shown in **Fig. 1e**. Data analysis was done as described⁴. The acquired G(τ) function was fitted by a one-component model as

$$G(\tau) = \frac{1}{N} \left(1 + \frac{\tau}{\tau_1} \right)^{-1} \left(1 + \frac{\tau}{s^2 \tau_1} \right)^{-1/2}$$

where τ₁ is the diffusion time of the fluorescent particles, N is the average number of fluorescent particles in the excitation-detection volume defined by the radius w₀ and length 2z₀, and s is the structure parameter representing the

ratio $s = z_0/w_0$. For quantitative evaluation, $G_c(0)$ (the amplitude of the cross-correlation function) is divided by $G_k(0)$ (the amplitude of the autocorrelation function of mKeima) to calculate the relative cross-correlation ($G_c(0)/G_k(0)$).

Monitoring the association between CaM and CaMKI. Recombinant proteins containing CaM/CaMKI and mKeima/CFP were generated using PROTEIOS, a wheat germ cell-free protein synthesis core kit (TOYOBO). The products were concentrated using VIVASPIN (VIVASCIENCE). Mixtures of two samples were analyzed by FCCS. The association between CaM and CaMKI was blocked by adding 0.1 mM EGTA and then achieved by adding 1 mM CaCl_2 .

Proteolysis analysis. mKeima-DEVD-CFP was expressed in *E. coli* and purified as previously described²³. The protein (10 nM) was incubated at 25 °C with activated caspase-3 (MBL) (0.2 U/ μl) in buffer containing 20 mM HEPES-KOH (pH 7.5), 10 mM KCl, 1.5 mM MgCl_2 , 1 mM EDTA, 1 mM EGTA and 1 mM dithiothreitol. Two days after transfection with the cDNA coding for mKeima-DEVD-CFP, HeLa cells in HBSS (Invitrogen) were treated with 100 ng/ml anti-Fas antibodies (CH-11; MBL) and cyclohexamide (10 $\mu\text{g}/\text{ml}$)²⁵.

Multicolor imaging. EGFP-go, YFP-mt, dKeima570-nu and mKeima-mit were constructed by fusing the 81 N-terminal amino acids of the type II membrane-anchored protein galactosyltransferase²⁶, the human wild-type tau four-repeat²⁷, the nuclear localization signal from poly(ADP-ribose) polymerase (S.K., T.A. and A.M., unpublished results) and the 29 N-terminal amino acids of the cytochrome *c* oxidase subunit VIII presequence²⁸ to the N termini of EGFP (Clontech), YFP, dKeima570 and mKeima, respectively. CFP-pm was generated by fusing the 20 C-terminal amino acids of K-Ras²⁹ to the C terminus of ECFP (Clontech). mMiCy-er was generated by extending mMiCy at the N terminus with the signal peptide from calreticulin and at the C terminus with an ER retention signal³⁰. cDNAs coding for the chimeric proteins were transfected into Vero cells using Lipofectamine 2000 (Invitrogen). Spectra imaging with a single laser line at 458 nm (Ar ion laser) was performed using the 32 channels of the LSM 510 META system (Carl Zeiss).

Accession codes. DNA Data Bank of Japan: the sequences reported in this paper have been deposited with accession nos. AB209967, AB209968 and AB209969.

Note: Supplementary information is available on the Nature Biotechnology website.

ACKNOWLEDGMENTS

The authors would like to thank K. Iwao and S. Hosaka at the Akajima Marine Science Laboratory for acquiring the stony coral animals, Y. Isogai for assistance with analytical centrifugation, F. Ishidate, K. Weissart, B. Zimmerman, Y. Hasegawa for assistance with FCCS measurements and spectral imaging, and K. Ishihara, H. Watanabe, T. Fukano, and M. Hirano for assistance with multi-color imaging and fluorescence lifetime measurements. This work was partly supported by grants from Japan MEXT Grant-in-Aid for Scientific Research on priority areas, NEDO (the New Energy and Industrial Technology Development Organization), HFSP (the Human Frontier Science Program), and RIKEN Strategic Research Program.

COMPETING INTERESTS STATEMENT

The authors declare competing financial interests (see the Nature Biotechnology website for details).

Published online at <http://www.nature.com/naturebiotechnology/>

Reprints and permissions information is available online at <http://npg.nature.com/reprintsandpermissions/>

- Kettling, U., Koltermann, A., Schwill, P. & Eigen, M. Real-time enzyme kinetics monitored by dual-color fluorescence cross-correlation spectroscopy. *Proc. Natl. Acad. Sci. USA* **95**, 1416–1420 (1998).

- Weidemann, T., Wachsmuth, M., Tewes, M., Rippe, K. & Langowski, J. Analysis of ligand binding by two-colour fluorescence cross-correlation spectroscopy. *Single Mol.* **3**, 49–61 (2002).
- Kim, S.A. & Schwill, P. Intracellular applications of fluorescence correlation spectroscopy: prospects for neuroscience. *Curr. Opin. Neurobiol.* **13**, 583–590 (2003).
- Saito, K., Wada, I., Tamura, M. & Kinjo, M. Direct detection of caspase-3 activation in single live cells by cross-correlation analysis. *Biochem. Biophys. Res. Commun.* **324**, 849–854 (2004).
- Kohl, T., Hauste, E. & Schwill, P. Determining protease activity in vivo by fluorescence cross-correlation analysis. *Biophys. J.* **89**, 2770–2782 (2005).
- Hwang, L.C. & Wohland, T. Single wavelength excitation fluorescence cross-correlation spectroscopy with spectrally similar fluorophores: Resolution for binding studies. *J. Chem. Phys.* **122**, 114708 (1–11) (2005).
- Martin, B.R., Giepmans, B.N., Adams, S.R. & Tsien, R.Y. Mammalian cell-based optimization of the biarsenical-binding tetracycline motif for improved fluorescence and affinity. *Nat. Biotechnol.* **23**, 1308–1314 (2005).
- Helmchen, F. & Denk, W. New developments in multiphoton microscopy. *Curr. Opin. Neurobiol.* **12**, 593–601 (2002).
- Heinze, K.G., Koltermann, A. & Schwill, P. Simultaneous two-photon excitation of distinct labels for dual-color fluorescence cross-correlation analysis. *Proc. Natl. Acad. Sci. USA* **97**, 10377–10382 (2000).
- Kohl, T., Heinze, K.G., Kuhlmann, R., Koltermann, A. & Schwill, P. A protease assay for two-photon cross-correlation and FRET analysis based solely on fluorescent proteins. *Proc. Natl. Acad. Sci. USA* **99**, 12161–12166 (2002).
- Heinze, K.G., Rarbach, M., Jahn, M. & Schwill, P. Two-photon fluorescence coincidence analysis: rapid measurements of enzyme kinetics. *Biophys. J.* **83**, 1671–1681 (2002).
- Kim, S.A., Heinze, K.G., Waxham, M.N. & Schwill, P. Intracellular calmodulin availability accessed with two-photon cross-correlation. *Proc. Natl. Acad. Sci. USA* **101**, 105–110 (2004).
- Patterson, G.H. & Piston, D.W. Photobleaching in two-photon excitation microscopy. *Biophys. J.* **78**, 2159–2162 (2000).
- Chen, T.S., Zeng, S.Q., Luo, Q.M., Zhang, Z.H. & Zhou, W. High-order photobleaching of green fluorescent protein inside live cells in two-photon excitation microscopy. *Biophys. Biochem. Res. Commun.* **291**, 1272–1275 (2002).
- Matz, M.V., Lukyanov, K.A. & Lukyanov, S.A. Family of the green fluorescent protein: journey to the end of the rainbow. *Bioessays* **24**, 953–959 (2002).
- Labas, Y.A. *et al.* Diversity and evolution of the green fluorescent protein family. *Proc. Natl. Acad. Sci. USA* **99**, 4256–4261 (2002).
- Tsutsui, H., Karasawa, S., Shimizu, H., Nukina, N. & Miyawaki, A. Semi-rational engineering of a coral fluorescent protein into an efficient highlighter. *EMBO Rep.* **6**, 233–238 (2005).
- Tsien, R.Y. The green fluorescent protein. *Annu. Rev. Biochem.* **67**, 509–544 (1998).
- Campbell, R.E. *et al.* A monomeric red fluorescent protein. *Proc. Natl. Acad. Sci. USA* **99**, 7877–7882 (2002).
- Crivici, A. & Ikura, M. Molecular and structural basis of target recognition by calmodulin. *Annu. Rev. Biophys. Biomol. Struct.* **24**, 85–116 (1995).
- Nagai, T., Yamada, S., Tominaga, T., Ichikawa, M. & Miyawaki, A. Expanded dynamic range of fluorescent indicators for Ca^{2+} by circularly permuted yellow fluorescent proteins. *Proc. Natl. Acad. Sci. USA* **101**, 10554–10559 (2004).
- Karasawa, S., Araki, T., Nagai, T., Mizuno, H. & Miyawaki, A. Cyan-emitting and orange-emitting fluorescent proteins as a donor/acceptor pair for fluorescence resonance energy transfer. *Biochem. J.* **381**, 307–312 (2004).
- Karasawa, S., Araki, T., Yamamoto-Hino, M. & Miyawaki, A. A green-emitting fluorescent protein from *Galaxiella* coral and its monomeric version for use in fluorescent labeling. *J. Biol. Chem.* **278**, 34167–34171 (2003).
- Sawano, A. & Miyawaki, A. Directed evolution of green fluorescent protein by a new versatile PCR strategy for site-directed and semi-random mutagenesis. *Nucleic Acids Res.* **28**, E78 (2000).
- Arcott, P.L. *et al.* Fas (CD95) expression is up-regulated on papillary thyroid carcinoma. *J. Clin. Endocrinol. Metab.* **84**, 4246–4252 (1999).
- Llopis, J., McCaffery, J.M., Miyawaki, A., Farquhar, M.G. & Tsien, R.Y. Measurement of cytosolic, mitochondrial, and Golgi pH in single living cells with green fluorescent proteins. *Proc. Natl. Acad. Sci. USA* **95**, 6803–6808 (1998).
- Sato, S. *et al.* Aberrant tau phosphorylation by glycogen synthase kinase-3 β and JNK3 induces oligomeric tau fibrils in COS-7 cells. *J. Biol. Chem.* **277**, 2060–2065 (2002).
- Sawano, A., Hama, H., Saito, N. & Miyawaki, A. Multicolor imaging of Ca^{2+} and protein kinase C signals using novel epifluorescence microscopy. *Biophys. J.* **82**, 1076–1085 (2002).
- Mochizuki, N. *et al.* Spatio-temporal images of growth-factor-induced activation of Ras and Rap1. *Nature* **411**, 1065–1068 (2001).
- Miyawaki, A. *et al.* Fluorescent indicator for Ca^{2+} based on green fluorescent proteins and calmodulin. *Nature* **388**, 882–887 (1997).